Application of the Hubbard model to $Cp^*_2Yb(bipy)$, a model system for strong exchange coupling in lanthanide systems

Wayne W. Lukens*, Nicola Magnani, and Corwin H. Booth

Chemical Sciences Division

Lawrence Berkeley National Laboratory

Berkeley, CA, 94720

KEYWORDS: single molecule magnet, Hubbard model, lanthanide, exchange coupling, magnetism

ABSTRACT: Exchange coupling is quantified in lanthanide (Ln) single molecule magnets (SMMs) containing a bridging N_2^{3-} radical ligand and between $[Cp^*_2Yb]^+$ and $bipy^{\bullet-}$ in $Cp^*_2Yb(bipy)$ where Cp* is pentamethylcyclopentadienyl and bipy is 2,2'-bipyridyl. In the case of these lanthanide SMMs, the magnitude of exchange coupling between the Ln ion and the bridging N_2^{3-}, 2J, is very similar to the barrier to magnetic relaxation, U_{eff}. A molecular version of the Hubbard model is applied to systems in which unpaired electrons on magnetic metal ions have direct overlap with unpaired electrons residing on ligands. The Hubbard model explicitly addresses electron correlation, which is essential for understanding the magnetic behavior of these complexes. This model is applied quantitatively to $Cp^*_2Yb(bipy)$ to explain its very strong exchange coupling, 2J = -0.11 eV (-920 cm^{-1}). The model is also used to explain the presence of strong exchange coupling in Ln SMMs in which the lanthanide spins are coupled *via* bridging N_2^{3-} radical ligands. The results suggest that increasing the magnetic coupling in lanthanide clusters could lead to an increase in the blocking temperatures of exchange-coupled lanthanide SMMs suggesting routes to the rational design of future lanthanide SMMs.

Introduction

Single molecule magnets (SMMs), which are isolated molecules that display slow magnetic relaxation, have been vigorously pursued as qubits for quantum computers,[1,2] molecular spin-valves,[3] and as interesting subjects for fundamental studies of molecular magnetism.[4,5] Perhaps the most important property of an SMM is its blocking temperature, below which the SMM displays hysteresis. This temperature represents the approximate upper limit for the operating temperature of any SMM-based device. A variety of approaches to increase the blocking temperature have been tried including increasing the spin of the SMM by incorporating multiple, exchange-coupled metal ions or increasing the magnetic anisotropy of the SMM by incorporating lanthanide (Ln) ions. However, using both strategies in the same SMM has proven difficult, as exchange coupling involving Ln ions is generally weak. In fact, typical Ln SMMs involve isolated Ln ions; for example, $[Pc_2Tb]^-$ and $\{[Pc(OEt)_8]_2Dy\}^-$ (PcH_2 = phthalocyanine) display magnetic hysteresis up to 1.7 K and 4 K, respectively.[6,7] A previous suggestion[3] that the addition of active radicals with unpaired electrons could result in higher blocking temperatures is consistent with recent reports for $\{[L_2(thf)Ln]_2(\mu-\eta^2:\eta^2-N_2)\}^-$, **1**, (L = $N(SiMe_3)_2$, thf = tetrahydrofuran), which display hysteresis to 8.3 K, and 14 K for Ln = Dy and Tb (**1-Dy** and **1-Tb**), respectively.[8,9] In contrast, the best transition metal SMM possesses hysteresis to 4.5 K.[10]

Single molecule magnetic behavior arises from an energy barrier, U_{eff}, (usually due to zero field splitting in transition metal clusters and to ligand field anisotropy in lanthanide and actinide complexes) that inhibits magnetization reversal in an applied field and "freezes" the magnetic state of the system. The magnetic relaxation time of an SMM, τ, is related to the energy barrier by an Arrhenius relationship, $\tau = \tau_0 \exp(U_{eff}/k_BT)$. Ideally, this thermal barrier determines the blocking temperature at which the hysteresis loop closes. However in most SMMs, lower energy pathways, especially tunneling through the barrier,[11] dominate relaxation behavior, and the blocking temperature is much lower than expected from U_{eff}.[6,12] For example, in the terbium phthalocyanine triple-decker complex $Tb_2(obPc)_3$, where obPc is the dianion of octabutoxyphthalocyanine, U_{eff} is comparable to that of **1-Tb**, but non-Arrhenius

relaxation pathways limit the blocking temperature to 1.5 K.[13] In contrast, the hysteresis loops of **1-Dy** and **1-Tb** close at temperatures consistent with the measured values of U_{eff} for these molecules. At the blocking temperature, the most important relaxation pathway in **1** appears to be thermally activated relaxation due to U_{eff}. At lower temperatures, other pathways, presumably tunneling pathways, are more important, and **1-Dy** and **1-Tb** undergo relaxation faster than predicted by the Arrhenius relationship.[8]

In **1**, the high blocking temperature is related to antiferromagnetic exchange coupling between each trivalent Ln ion and the bridging dinitrogen radical, which gives rise to a molecular ferrimagnet in which the moments of the Ln ions are aligned with each other and anti-aligned with the moment of the bridging N_2^{3-} radical. The role of the bridging dinitrogen radical may be inferred by the absence of SMM properties in **2**, in which the closed-shell dinitrogen ligand forms a bridge between the two Ln fragments (see Figure 1).[9] While strong exchange coupling between the magnetic ions appears necessary to produce high blocking temperatures in these SMMs, strong exchange coupling alone cannot guarantee high blocking temperatures since other relaxation pathways could decrease the blocking temperature. Nevertheless, understanding the origin of the strong exchange coupling between Ln^{3+} and N_2^{3-} is a crucial first step towards rationally designing Ln SMMs with stronger exchange coupling.

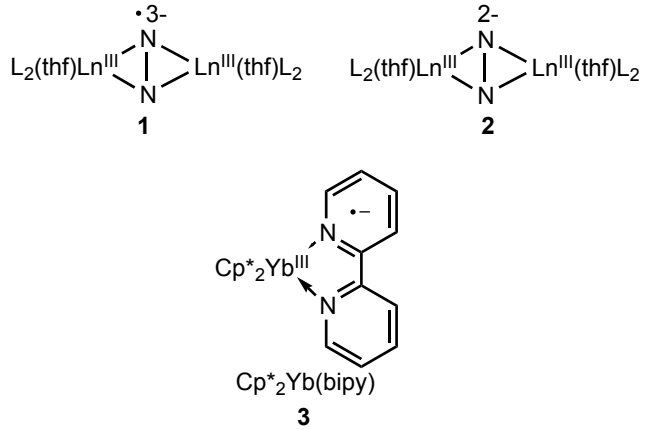

Figure 1. Molecules discussed in this paper. Cp* is pentamethylcyclopentadienyl, bipy is 2,2'-bipyridine, L is $N(SiMe_3)_2$, and thf is tetrahydrofuran. In all cases, the lanthanide ion is trivalent.

Ideally, one would like to examine strong exchange in **1**; however, their complex magnetic behavior makes separating the effects of magnetic exchange from other effects difficult. Fortunately, similarly strong magnetic-coupling occurs in other Ln complexes. In particular, $Cp^*_2Yb(bipy)$, **3**, where Cp* is pentamethylcyclopentadienyl and bipy is 2,2'-bipyridine, displays, as does **1**, strong exchange coupling between a ligand-based radical and a trivalent Ln center.[14-17]

Previous studies have shown that **3** is multiconfigurational.[15,16] The main configuration, $|f^{13},bipy^{\bullet-}\rangle$, consists of a $[Cp^*_2Yb]^+$ fragment coordinated by a bipy radical anion ($bipy^{\bullet-}$). The minor configuration, $|f^{14},bipy\rangle$, consists of a neutral Cp^*_2Yb coordinated by a neutral bipy ligand. Overall, the wave function may be written as $\Psi = c_1 |f^{13},bipy^{\bullet-}\rangle + c_2 |f^{14},bipy\rangle$, where c_1 and c_2 are coefficients of the two configurations and $c_1^2 = 0.83$.[16] Computational modeling showed that the multiconfigurational ground state is due to mixing of low-lying excited states into the ground state.[15] The calculated stabilization of the singlet state is 0.28 eV, which suggests that exchange coupling should be very large in this system (the magnitude of the exchange coupling is equivalent to the stabilization of the singlet state in this case). However, quantifying exchange coupling between $bipy^{\bullet-}$ and the Yb^{3+} center has proven problematic due to the difficulty in modeling the magnetic susceptibility of exchange-coupled systems involving Ln ions.[18] While it is possible to model the variable temperature magnetic susceptibility of two identical, exchange-coupled Ln ions,[19] no analogous method currently exists for modeling the magnetic susceptibility of a Ln ion coupled to a non-identical spin such as an organic radical. However, the exchange coupling between Yb^{3+} and $bipy^{\bullet-}$ can be quantified from the temperature-independent paramagnetism (TIP) of the open-shell singlet ground state by extending the approach developed by Griffith[20] to metal ions with unquenched orbital angular momentum.

The strong exchange coupling in **3** may be quantitatively explained using a Hubbard-molecule model (HMM),[21,22] which is the well-known Hubbard model[23] applied to a single molecule. The HMM is bonding model that explicitly includes electron correlation, and can be thought of as an extension of

Hückel theory with an additional parameter for the electron pairing energy.[24] As a result, the HMM includes the effect of configuration interaction on the energies and wave functions of the electronic states of the molecule, which is essential to understand the behavior of **3** as demonstrated by the previous computational study.[15] The HMM has been used previously to model π-bonding in ethylene[24,25] and to quantify exchange coupling in donor-acceptor systems.[26] A similar configuration interaction model has been used as part of a larger Hamiltonian to understand covalency in Cp_3Yb.[27] In addition, Hubbard developed a related model for covalency in transition metal complexes, where the main difference is that Hubbard's transition metal model addresses interactions with closed shell ligands while the HMM addresses interactions with ligands containing unpaired electrons.[28]

In this paper, exchange coupling in **1** and **3** is quantified by extending the spin-only Heisenberg, Dirac, van Vleck (HDVV) Hamiltonian to metal ions with unquenched orbital angular momentum. In **1**, the exchange coupling is shown to be very similar to U_{eff}. The very strong exchange coupling in **3** is explained quantitatively using the HMM. The HMM is also used to explain why the exchange coupling in **1** and **3** is much larger than in other lanthanide complexes with radical-based ligands.

Results and discussion

Exchange coupling in Lanthanide Single Molecule Magnets (1)

The previous studies by Rinehart, et al., clearly demonstrate that exchange coupling is necessary for SMM behavior of **1**;[8,9] therefore, estimating the magnitude of this exchange coupling would be useful to better understand its effect on the magnetic relaxation of these molecules. Only the value for the Gd-based complex was determined in Ref. 9 using a Heisenberg-Dirac-van Vleck (HDVV) Hamiltonian of the form $\mathcal{H} = -2J(\mathbf{S}_1+\mathbf{S}_2)\bullet\mathbf{S}_r$, where J is the effective exchange constant, $\mathbf{S}_1$ and $\mathbf{S}_2$ are the spin momenta of the two rare-earth ions, and $\mathbf{S}_r$ is the spin of the radical (an intermolecular interaction was also taken into account, but it is extremely weak and we will neglect it here).

In principle, the same Hamiltonian describes the exchange interaction in **1** for other rare earths; however, the situation is complicated by the presence of the orbital moment, **L**, along with the spin, so that a significant influence of the ligand field (LF) potential is expected, which ultimately results in highly anisotropic coupling between the total angular momenta of the lanthanide ions and the spin of the radical. Fortunately, important conclusions regarding the exchange interaction can be inferred by studying the susceptibility curve measured for **2** (the variant of **1** with a magnetically inactive N_2^{2-} radical and negligible exchange between the two Dy ions). In particular, the magnetic moments of **2** are very close to the free-ion values above 150 K, which implies that the energy levels corresponding to the LF-split ground multiplet are all thermally populated above this temperature. We can therefore safely assume that the crystal-field effect on the susceptibility of **1** will also be weak in this temperature range and that it can be accounted for by a scaling factor equal to the ratio between the measured susceptibility for **2** and its theoretical value for two uncoupled free ions (in other words, by varying the effective Landé g factor, g_{eff}). We then calculate the susceptibility curve by numerical diagonalization of the HDVV Hamiltonian within the whole subspace defined by the ground multiplets of the two Ln ions (*e.g.*, the $^6H_{15/2}$ multiplet for Dy) and the $S_{rad} = 1/2$ spin moment of the radical, using the projection $\mathbf{S} = (g_{eff}-1)\boldsymbol{J}$ to give $\mathcal{H} = -2J(g_{eff}-1)(\boldsymbol{J}_1+\boldsymbol{J}_2)\bullet\mathbf{S}_r$, where $\boldsymbol{J}_1$ and $\boldsymbol{J}_2$ are the total angular momenta of the two rare earth ions ($\boldsymbol{J} = \mathbf{L} + \mathbf{S}$).[29,30] The best fits to the experimental data published in Refs. 8 and 9 are shown in Figure 2, and were obtained using the parameters given in Table 1. The values obtained for g_{eff} do not significantly deviate from the Landé g-values, g_J, for the free trivalent rare earth ions.

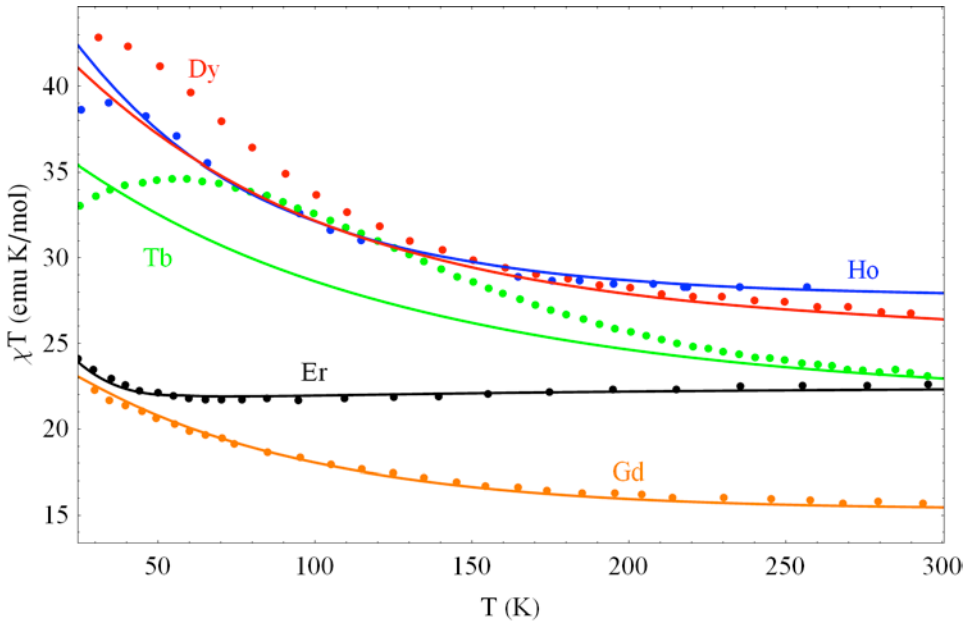

Figure 2. Experimental (dots) and calculated (lines) magnetic susceptibility for **1**. All experimental data were taken from Refs. 8 and 9.

Table 1. The values of g_{eff} and 2J obtained from the fits presented in Figure 2. The Landé g-values and the barrier for magnetic relaxation U_{eff} from Refs. 9 and 8 are included for comparison.

Ln	g_{eff}	2J (cm^{-1})	g_J	U_{eff} (cm^{-1})
Er	1.18	21	1.20	36
Ho	1.25	83	1.25	73
Dy	1.28	102	1.33	123
Tb	1.45	(108)[a]	1.50	227
Gd	2.00[b]	54	2.00[b]	–

a) Modeled susceptibility does not agree with the data for Tb as discussed in the text.
b) Fixed at g=2.00

As shown in Figure 2, the calculated susceptibility is in good agreement with the experimental values for **1-Er**, **1-Ho**, and **1-Dy**, and Table 1 shows that the values of 2J and U_{eff} are similar for these compounds. Since 2J represents the energy gap between the two lowest-lying spin states, this result suggests that the magnetic relaxation pathway in these complexes may be due to loss of the exchange interaction. Hence, the strength of the coupling between the Ln and the bridging N_2^{3-} may determine the magnetic relaxation rate, which ultimately determines the blocking temperature in these complexes. On the other hand, we were unable to obtain a satisfactory fit for **1** with M = Tb (**1-Tb)** with our HDVV calculations, and the susceptibility curves for **2-Tb** show a significant influence from the ligand-field potential, which is not particularly surprising since Tb complexes often display large energy gaps between states (e.g., first excited state of $[Pc_2Tb]^-$ is roughly 400 cm^{-1} above the ground state).[7] For this

reason, the value of 2J for **1-Tb** is not reliable and cannot be directly compared to U_{eff}. It is also possible that the high barrier in **1-Tb** (227 cm^{-1}) is due at least in part to other mechanisms not considered in the present study, such as Orbach transitions to higher-lying ligand-field states.[18,31]

These results suggest that the U_{eff} in **1** may be due to exchange coupling between the lanthanide ions and the bridging N_2^{3-} radical, but these results do not explain why other relaxation pathways in **1** appear to be suppressed. Previous investigations have observed that exchange coupling can enhance SMM behavior in Ln complexes.[12,32-36]

Exchange coupling in $Cp^*_2Yb(bipy)$ (3)

Since exchange coupling in **1** is intimately related to its SMM behavior, understanding why exchange coupling in **1** is so much stronger than typically encountered in lanthanide systems would be useful. However, the SMM behavior of **1** complicates this investigation; therefore, the origin of very strong exchange coupling between a Ln-ion and an organic radical was studied in a different system, **3**, with the goal of applying the information gained about **3** to explain the strong exchange coupling in **1**. As noted in the introduction, **3** has been extensively studied and shown to have a singlet ground state with a large energy gap to the excited triplet state.[15] At low temperatures, **3** is best described as a temperature independent paramagnet with χ_{TIP} = 0.0016(2) emu where the error given in parentheses reflects the difficulty in determining the value of χ_{TIP} in the presence of the "Curie tail" (paramagnetic contribution due to the presence of impurities). The temperature independent magnetism (TIP) of **3** results from the unquenched orbital angular momentum of the electron on the Yb(III) center. Consequently, **3** is quite paramagnetic: the TIP is approximately 2 Bohr magneton at room temperature.

If spin-orbit coupling was insignificant in **3**, 2J could be determined from χ_{TIP} using eqn 1,[20] where c_1 is the coefficient for the $|f^{13},bipy^{\bullet-}\rangle$ configuration that gives rise to the TIP, N is Avogadro's number, β is the Bohr magneton, g_i are the g-values for Yb^{3+} in **3**, and $g_{bipy^{\bullet-}}$ is the g-value of $bipy^{\bullet-}$.

$$\chi_{TIP} \cong c_1^2 \frac{N\beta^2}{12J} \sum_{i=x,y,z} (g_i - g_{bipy^{\bullet-}})^2 \quad (1)$$

Equation 1 is appropriate for the spin-only Heisenberg, Dirac, van Vleck (HDVV) spin Hamiltonian, $\mathcal{H}=-2J\mathbf{S}_{Yb3+}\bullet\mathbf{S}_{bipy\bullet-}$. Since **3** posses unquenched orbital angular momentum, eqn 1 is not directly applicable but can be used once the presence of unquenched orbital angular momentum is taken into account. To accomplish this, the spin of Yb^{3+} is first projected onto its total angular momentum, $\boldsymbol{J}_{Yb3+}$, as was done for **1**, using $\mathbf{S}_{Yb3+} = (g_J-1)\boldsymbol{J}_{Yb3+}$, which gives $\mathcal{H}= -(g_J-1)2J\boldsymbol{J}_{Yb3+}\bullet\mathbf{S}_{bipy\bullet-}$.[29,30] Due to the unquenched orbital angular momentum of **3**, the coupling between $\boldsymbol{J}_{Yb3+}$ and $\mathbf{S}_{bipy\bullet-}$ is highly anisotropic. For the ground Kramer's doublet of Yb^{3+} in **3**, $g_J\boldsymbol{J}_{Yb3+} = \mathbf{g}_{Yb3+}\bullet\widetilde{\mathbf{S}}_{Yb3+}$ where $\mathbf{g}_{Yb3+}$ and $\widetilde{\mathbf{S}}_{Yb3+}$ are the g-tensor and effective spin for the ground Kramer's doublet, respectively, and the Hamiltonian may be written as $\mathcal{H}=-2J[(g_J-1)/g_J](\mathbf{g}_{Yb3+}\bullet\widetilde{\mathbf{S}}_{Yb3+})\bullet\mathbf{S}_{bipy\bullet-}$.[30] In this way, the anisotropy in the exchange may be expressed in terms of measurable quantities, the EPR g-values of the ground Kramers's doublet of the Yb^{3+} fragment. The corresponding relationship between χ_{TIP} and J is given by eqn 2.

$$\chi_{TIP} \cong c_1^2 \frac{N\beta^2}{12J} \sum_{i=x,y,z} \frac{g_J(g_i - g_{bipy^{\bullet-}})^2}{g_i(1-g_J)} \quad (2)$$

Although the g-values for Yb^{3+} spins in **3** cannot be readily determined, those of the closely related complex $[Cp^*_2Yb(bipy)]^+I^-$ ($\mathbf{3^+I^-}$) are 7.050, 1.731, and 1.165.[19] Since the structures of $\mathbf{3^+I^-}$ and **3** are almost identical, the complexes must have similar ligand fields, and the g-values of $\mathbf{3^+I^-}$ should be good estimates for those of **3**. In this way, the information about the ligand field and unquenched orbital angular momentum of **3** needed for eqn 2 is obtained from its diamagnetic substitute, $\mathbf{3^+I^-}$.[19,37] Using χ_{TIP} and the g-values of $\mathbf{3^+I^-}$, eqn 2 yields 2J = -0.11(2) eV or -920(180) cm^{-1}. This surprisingly large value is consistent with the large value predicted computationally.[15]

Hubbard-molecule model

The exchange coupling in **3** is approximately three orders of magnitude larger than exchange coupling in typical lanthanide systems as well as an order of magnitude greater than in **1**. The previous computational study clearly shows that both the strong exchange coupling in **3** and its multiconfigurational ground state are related to the mixing of low-lying singlet states into the ground state. The strong exchange coupling in **3** may be quantitatively explained using a Hubbard-molecule model (HMM).[21,22] The HMM includes two sites, two electrons and two parameters: t and U. The transfer integral, t, determines how readily a single electron may move between the two sites and is the stabilization of the bonding orbital due to the overlap of the orbitals containing the unpaired electrons (t is equivalent to -β in the Hückel model for π-electrons).[23] Electron repulsion, U, is the energy needed to pair the electrons on a single site and is closely related to charge transfer within the molecule.

The HMM allows t and U to be determined spectroscopically, so that the extent of exchange coupling predicted by the HMM may be compared with that determined from the TIP of **3**. In the case of **3**, the ligand-field potential isolates a doublet ground state ($\widetilde{\mathbf{S}}_{\mathbf{Yb3+}} = 1/2$) for the $4f^{13}$ configuration of Yb^{3+}, and the HMM basis set includes the six states shown in Figure 3. Following the recent work on covalency in Cp_3Yb,[27] states Ψ_1-Ψ_4 describe ionic bonding in which the charges are localized on $Cp^*_2Yb^+$ and $bipy^{\bullet-}$. State Ψ_5 describes covalent bonding in which an electron on $bipy^{\bullet-}$ has been shared with $Cp^*_2Yb^+$. State Ψ_6 describes covalent bonding where an electron on $Cp^*_2Yb^+$ has been shared with the $bipy^{\bullet}$; however, Ψ_6 is at very high energy because it involves a tetravalent Yb ion, so Ψ_6 will not be used below. Likewise, the Yb^{3+} 5d-orbitals are much higher in energy and do not contribute significantly to the behavior of **1** apart from hybridizing with the 4f-orbitals to improve their overlap with the ligand orbitals (the single, half-occupied orbital labeled "4f" in Figure 3 is actually a 4f-5d hybrid orbital). In the absence of any interaction between the spin on the Yb^{3+} ion and the $bipy^{\bullet-}$ radical (*i.e.*, when t = 0), states Ψ_1 through Ψ_4 are degenerate and Ψ_5 is greater in energy by U, the energy needed to pair the electrons on the Yb center. The Hamiltonian for the system in which the Yb^{3+} and $bipy^{\bullet-}$ do not interact,

$\mathcal{H}_0$, can be written as $\mathcal{H}_0 = \mathcal{H}_{Yb3+} + \mathcal{H}_{bipy^{\bullet-}}$, where $\mathcal{H}_{Yb3+}$ and $\mathcal{H}_{bipy^{\bullet-}}$ are the Hamiltonians for the unpaired electrons on the isolated Yb^{3+} and $bipy^{\bullet-}$ fragments, respectively.

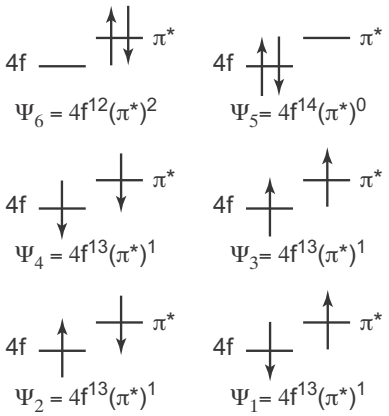

Figure 3. Electronic states that form the basis for the Hubbard-molecule model for $Cp^*_2Yb(bipy)$. The 4f-orbital corresponds to the single half-occupied 4f-orbital of Yb^{3+}, and the π* is the lowest lying antibonding orbital of bipy ligand, which is also half-occupied.

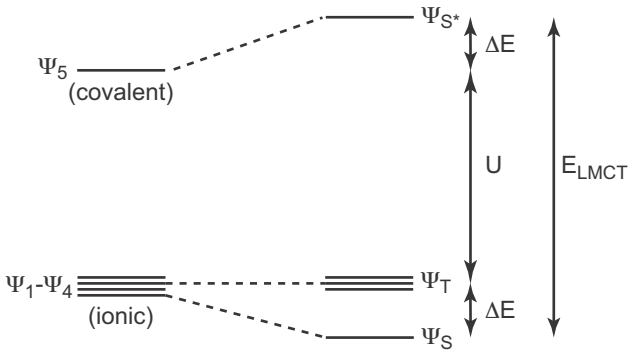

Figure 4. Energy levels in Hubbard molecule model for $Cp^*_2Yb(bipy)$. States on the left have no interaction between the Yb^{3+} and $bipy^{\bullet-}$ spins; states on the right result from including that interaction.

Allowing the spins on the bipy radical and Yb^{3+} center to interact produces the perturbed Hamiltonian $\mathcal{H}_1 = \mathcal{H}_0 + \mathcal{h}_1$ where $\mathcal{h}_1$ contains the interactions between the Yb^{3+} and $bipy^{\bullet-}$ fragments (the Hamiltonian for the HMM is given in the SI). These interactions allow the mixing of Ψ_5 into Ψ_1-Ψ_4, which lifts the degeneracy of states Ψ_1-Ψ_4 and destabilizes Ψ_5 as illustrated in Figure 4. Perturbation theory allows 2J

to be expressed in terms of t and U: $2J = \Delta E = -2t^2/U$, where $t = \langle \Psi_{Yb3+} | \hat{h}_1 | \Psi_{bipy\bullet-} \rangle$ and $U = \langle \Psi_1 | \hat{\mathcal{H}}_0 | \Psi_1 \rangle - \langle \Psi_5 | \hat{\mathcal{H}}_0 | \Psi_5 \rangle$. To first order, the resulting singlet, ground-state wave function, Ψ_S, is given in eqn 3.

$$\Psi_S = c\left[\left(\frac{1}{\sqrt{2}}\right)(\Psi_1 - \Psi_2) + \sqrt{2}\left(\frac{t}{U}\right)\Psi_5\right], \quad \frac{1}{c} = \sqrt{1 + 2\left(\frac{t}{U}\right)^2} \qquad (3)$$

As in the computational model, the ground state is multiconfigurational and can be described as a largely ionic bond, where c is the ionic character in the wave function, which also contains small amount of covalent character due to Ψ_5. In this case, the exchange coupling, 2J, is also the strength of the covalent interaction, ΔE. The relationship between the strength of the exchange coupling and the HMM parameters t and U is straightforward: increasing t (by increasing the overlap between the orbitals containing the unpaired electrons, for example) or decreasing U (by making the radical more strongly reducing, for example) strengthens the exchange coupling.

Analysis of exchange coupling in $Cp^*_2Yb(bipy)$ using the HMM

The HMM decouples the Hamiltonian that gives rise to the electronic structures of $[Cp^*_2Yb]^+$ and $bipy^{\bullet-}$, $\hat{\mathcal{H}}_0$, from the perturbation, $\hat{h}_1$, that contains the interactions between the spins on the two fragments. This decoupling allows the interaction between the spins on $Cp^*_2Yb^+$ and $bipy^{\bullet-}$ to be evaluated without knowing the details of the electronic structures of either fragment. In practice, this means that the interactions between the spins can be evaluated without knowing the crystal field parameters for **3**, which is important since its low symmetry makes evaluating the crystal field parameters extremely difficult. Using this approach allows t and U to be determined from previous spectroscopic studies of **3**.

As noted in the introduction, the wave function of **3** may be written as $\Psi = c_1 | f^{13}, bipy^{\bullet-} \rangle + c_2 | f^{14}, bipy \rangle$, where c_1 and c_2 are coefficients of the two configurations. X-ray absorption near-edge spectroscopy shows that **3** is multiconfigurational with c_1^2 equal to 0.83(3).[16] The absorption spectra of **3** and related

complexes have been extensively studied, and a low-lying transition at 4750(250) cm^{-1} has been assigned as a ligand-to-metal charge transfer band (E_{LMCT}).[38] Using these values of c_1^2 and E_{LMCT}, t and U are 0.13(1) eV and 0.42(4) eV, respectively, since $c_1^2 = c^2$ in eqn 3, and $E_{LMCT} = U + 4J = U+4(t/U)^2$ (see Figure 4). The resulting value of 2J is -0.09(1) eV or -700(90) cm^{-1}, which is in good agreement with the value of -0.11(2) eV determined from the susceptibility of **3.**

The value of t/U determined using perturbation theory is large, 0.32(1), which calls into question the validity of the perturbative solution. Therefore, the HMM was also solved exactly; the ground state, Ψ_S, is given in eqn 4, and ΔE is given in eqn 5.

$$\Psi_S = c\left[\frac{1}{\sqrt{2}}(\Psi_1 - \Psi_2) + \frac{U-\sqrt{U^2+8t^2}}{2\sqrt{2}t}\Psi_5\right]$$
$$\frac{1}{c} = \sqrt{1+\frac{\left(U-\sqrt{U^2+8t^2}\right)^2}{8t^2}} \qquad (4)$$

$$\Delta E = \frac{U-\sqrt{U^2+8t^2}}{2} \qquad (5)$$

The values of t, U, and 2J may be determined numerically to give t = 0.16(2) eV, U = 0.39(2) eV, and 2J = -0.10(2) eV, which are similar to the perturbative solution but in better agreement with the value determined from the TIP of **3**. While the exact solution seems more accurate, the perturbative solution allows a more intuitive understanding of the relationship between t and U and 2J.

The value of 2J predicted by the HMM is in good agreement with that determined experimentally. More importantly, the HMM underscores the intimate relationship between the strong exchange coupling and the multiconfigurational behavior of **3** and is illustrated in a simple manner. In **3**, configuration interaction is strong, due largely to the small value of U. This interaction results in substantial mixing of covalent Ψ_5 into the otherwise ionic bond between $[Cp^*_2Yb]^+$ and $bipy^{\bullet-}$. The strength of the covalent interaction is 2J.

Implication of the HMM for exchange coupling in lanthanide single molecule magnets

The HMM can also be used to understand the strong exchange coupling between the dinitrogen radical, N_2^{3-}, and each Ln center in **1**. The primary reason that exchange coupling in **1** is so much larger than in **2** is that coupling between N_2^{3-} radical and the Ln centers in **1** is due to the direct overlap of the orbitals containing the unpaired electrons, while coupling between the two Ln centers bridged by closed-shell N_2^{2-} in **2** is due to superexchange (i.e., there is no direct overlap of the orbitals containing unpaired spins). This difference is best illustrated by noting that exchange coupling in **1-Gd** is approximately 50 times stronger than in **2-Gd**. This effect has been observed previously for transition metal ions bridged by chloranilate dianion (CA^{2-}) and $CA^{\bullet 3-}$, where the interaction with the bridging radical ligand was much stronger than superexchange via the closed shell CA^{2-} ligand.[39,40] A recent DFT study of **1-Gd** reaches similar conclusions about the role of the bridging radical in this complex.[41]

While direct overlap between the Ln orbitals and the orbitals containing the unpaired electron is important, it is not sufficient to explain the strong exchange coupling in **1**. Direct overlap is also possible in Ln complexes containing stable radicals such as nitroxyl, yet these complexes display much weaker exchange coupling.[42-47] The HMM clearly explains why exchange coupling in **1** and **3** is strong while exchange coupling between Ln centers and ligands containing stable radicals such nitroxyl radicals is much weaker.[42-47] Trivalent lanthanide ions have large, negative reduction potentials, so strongly reducing ligands with similarly large, negative reductions potentials are needed to minimize U. Both N_2^3 and $bipy^{\bullet -}$ are strongly reducing, so U should be relatively small in **1** and **3**. In complexes with stable radical ligands, U will be much larger because these radicals are not strongly reducing.

The HMM not only explains the strong exchange coupling in **1**; it also illustrates a subtler but equally interesting effect. As shown in Table 1, the exchange coupling of **1-Dy** is roughly twice that of **1-Gd**. While this may seem counterintuitive (Gd has a larger pure-spin moment than Dy, and the 4f electrons

have a larger radial extent in **1-Gd** relative to **1-Dy** due of the Ln contraction), an obvious explanation can be found within the HMM: Dy^{2+} is more stable than Gd^{2+}, so U must be smaller in **1-Dy** than in **1-Gd**, and N_2^{3-} is more effective in creating exchange pathways in Dy than in Gd complexes.

Conclusion

The strong exchange coupling observed between lanthanides and strongly reducing radical ligands in **1** and **3** has been quantified. The similarity of the value of 2J for **1-Dy**, **1-Ho**, and **1-Er** to their thermal relaxation barrier, U_{eff}, suggests that the exchange coupling in **1** is an important factor in determining the behavior of these complexes, including the blocking temperature. The exchange coupling in both **1** and **3** is very large, and can be explained using a HMM. For **3**, the good correspondence between the level scheme derived from spectroscopic data and that determined using magnetic susceptibility shows that this model can accurately describe the singlet-triplet gap in lanthanide complexes displaying strong exchange coupling. The HMM illustrates in a simple manner how configuration interaction introduces covalency into an otherwise ionic bond through strong electron correlation. The HMM expresses the strength of this covalent interaction, 2J, in terms of t and U, which can be readily determined spectroscopically.

The HMM suggests two approaches to maximize exchange coupling in Ln systems. Matching the redox properties of the radical and the Ln can minimize U. Due to the large, negative reduction potentials of the Ln^{3+} ions, strongly reducing radical ligands should lower the value of U, especially when coupled to lanthanides that have accessible divalent states (Nd, Eu, Sm, Dy, Tm, and Yb). Likewise, strongly oxidizing ligands may lower the value of U for lanthanides that have accessible tetravalent states (Ce, Pr, and Tb). In addition, increasing the overlap between the radical ligand and the metal ion can increase t, which might be accomplished through the use of actinide ions, where the radial extent of the 5f-orbitals is greater than the radial extent of the Ln 4f-orbitals. In any case, the exchange coupling found in **3**, 920 cm^{-1}, shows that strong magnetic exchange is possible for Ln ions and that the coupled state

may persist to relatively high temperatures. In comparison, the coupling in **1-Dy** is approximately an order of magnitude weaker than in **3**, which suggests that the exchange coupling in Ln-cluster SMMs can be increased substantially.

Acknowledgements

The authors thank Richard Andersen for many helpful discussions about the chemistry and magnetism of organometallic complexes, especially **3**, and for a critical review of this manuscript. The authors gratefully acknowledge the support of the Lawrence Berkeley National Laboratory LDRD program. This work was supported by the Director, Office of Science, of the U.S. Department of Energy under Contract No. DE-AC02-05CH11231.

Supporting information available: Hamiltonian for the HMM.

References

1. Lehmann, J.; Gaita-Arino, A.; Coronado, E.; Loss, D. *Nat. Nanotechnol.* **2007**, *2*, 312.
2. Leuenberger, M. N.; Loss, D. *Nature* **2001**, *410*, 789.
3. Bogani, L.; Wernsdorfer, W. *Nat. Mater.* **2008**, *7*, 179.
4. Gatteschi, D.; Sessoli, R. *J. Magn. Magn. Mater.* **2004**, *272*, 1030.
5. Gatteschi, D.; Caneschi, A.; Pardi, L.; Sessoli, R. *Science* **1994**, *265*, 1054.
6. Ishikawa, N.; Mizuno, Y.; Takamatsu, S.; Ishikawa, T.; Koshihara, S. Y. *Inorg. Chem.* **2008**, *47*, 10217.
7. Ishikawa, N.; Sugita, M.; Ishikawa, T.; Koshihara, S.; Kaizu, Y. *J. Phys. Chem. B* **2004**, *108*, 11265.
8. Rinehart, J. D.; Fang, M.; Evans, W. J.; Long, J. R. *J. Am. Chem. Soc.* **2011**, *133*, 14236.
9. Rinehart, J. D.; Fang, M.; Evans, W. J.; Long, J. R. *Nat. Chem.* **2011**, *3*, 538.
10. Milios, C. J.; Vinslava, A.; Wernsdorfer, W.; Moggach, S.; Parsons, S.; Perlepes, S. P.; Christou, G.; Brechin, E. K. *J. Am. Chem. Soc.* **2007**, *129*, 2754.
11. Aubin, S. M. J.; Ruiz, D.; Rumberger, E.; Sun, Z.; Albela, B.; Wemple, M. W.; Dilley, N. R.; Ribas, J.; Maple, B. M.; Christou, G.; Hendrickson, D. N. *Mol. Cryst. Liq. Cryst.* **1999**, *335*, 371.
12. Sessoli, R.; Powell, A. K. *Coord. Chem. Rev.* **2009**, *253*, 2328.
13. Katoh, K.; Kajiwara, T.; Nakano, M.; Nakazawa, Y.; Wernsdorfer, W.; Ishikawa, N.; Breedlove, B. K.; Yamashita, M. *Chem. Eur. J* **2011**, *17*, 117.
14. Walter, M. D.; Berg, D. J.; Andersen, R. A. *Organometallics* **2006**, *25*, 3228.
15. Booth, C. H.; Walter, M. D.; Kazhdan, D.; Hu, Y. J.; Lukens, W. W.; Bauer, E. D.; Maron, L.; Eisenstein, O.; Andersen, R. A. *J. Am. Chem. Soc.* **2009**, *131*, 6480.
16. Booth, C. H.; Walter, M. D.; Daniel, M.; Lukens, W. W.; Andersen, R. A. *Phys. Rev. Lett.* **2005**, *95*, 267202.

17. Schultz, M.; Boncella, J. M.; Berg, D. J.; Tilley, T. D.; Andersen, R. A. *Organometallics* **2002**, *21*, 460.
18. Palii, A.; Tsukerblat, B.; Klokishner, S.; Dunbar, K. R.; Clemente-Juan, J. M.; Coronado, E. *Chem. Soc. Rev.* **2011**, *40*, 3130.
19. Lukens, W. W.; Walter, M. D. *Inorg. Chem.* **2010**, *49*, 4458.
20. Griffith, J. S. In *Structure and Bonding* Springer Verlag: New York, 1972; Vol. 10.
21. Sousa, M. C. B.; Maced, C. A. *Scientia Plena* **2008**, *4*, 094401.
22. Chiappe, G.; Louis, E.; SanFabian, E.; Verges, J. A. *Phys. Rev. B* **2007**, *82*, 1.
23. Hubbard, J. *Proc. Roy. Soc. A* **1963**, *276*, 238.
24. Fox, M. A.; Matsen, F. A. *J. Chem. Educ.* **1985**, *62*, 367.
25. Matsen, F. A. *Int. J. Quantum Chem.* **1976**, *10*, 511.
26. Weiss, E. A.; Wasielewski, M. R.; Ratner, M. A. *J. Chem. Phys.* **2005**, *123*, 8.
27. Denning, R. G.; Harmer, J.; Green, J. C.; Irwin, M. *J. Am. Chem. Soc.* **2011**, *133*, 20644.
28. Hubbard, J.; Rimmer, D. E.; Hopgood, F. R. A. *Proc. Roy. Soc.* **1966**, *88*, 13.
29. Birgeneau, R.; Hutchings, M.; Baker, J.; Riley, J. *J. Appl. Phys.* **1969**, *40*, 1070.
30. Abragam, A.; Bleaney, B. *Electron Paramagnetic Resonance of Transition Ions*; Clarendon Press: Oxford, 1970.
31. Sorace, L.; Benelli, C.; Gatteschi, D. *Chem. Soc. Rev.* **2011**, *40*, 3092.
32. Long, J.; Habib, F.; Lin, P.-H.; Korobkov, I.; Enright, G.; Ungur, L.; Wernsdorfer, W.; Chibotaru, L. F.; Murugesu, M. *J. Am. Chem. Soc.* **2011**, *133*, 5319.
33. Costes, J.-P.; Shova, S.; Wernsdorfer, W. *Dalton Trans.* **2008**, 1843.
34. Lopez, N.; Prosvirin, A. V.; Zhao, H.; Wernsdorfer, W.; Dunbar, K. R. *Chem. Eur. J* **2009**, *15*, 11390.
35. Coronado, E.; Giménez-Saiz, C.; Recueno, A.; Tarazón, A.; Romero, F. M.; Camón, A.; Luis, F. *Inorg. Chem.* **2011**, *50*, 7370.
36. Hewitt, I. J.; Tang, J.; Madhu, N. T.; Anson, C. E.; Lan, Y.; Luzon, J.; Etienne, M.; Sessoli, R.; Powell, A. K. *Angew. Chem. Int. Ed.* **2010**, *49*, 6352.
37. Costes, J. P.; Dahan, F.; Dupuis, A.; Laurent, J. P. *Chem.-Eur. J.* **1998**, *4*, 1616.
38. Da Re, R. E.; Kuehl, C. J.; Brown, M. G.; Rocha, R. C.; Bauer, E. D.; John, K. D.; Morris, D. E.; Shreve, A. P.; Sarrao, J. L. *Inorg. Chem.* **2003**, *42*, 5551.
39. Min, K. S.; DiPasquale, A. G.; Golen, J. A.; Rheingold, A. L.; Miller, J. S. *J. Am. Chem. Soc.* **2007**, *129*, 2360.
40. Dei, A.; Gatteschi, D.; Pardi, L.; Russo, U. *Inorg. Chem.* **1991**, *30*.
41. Rajeshkumar, T.; Rajaraman, G. *Chem. Commun.* **2012**, *48*, 7856.
42. Caneschi, A.; Dei, A.; Gatteschi, D.; Poussereau, S.; Sorace, L. *Dalton Trans.* **2004**, 1048.
43. Benelli, C.; Caneschi, A.; Gatteschi, D.; Pardi, L.; Rey, P.; Shum, D. P.; Carlin, R. L. *Inorg. Chem.* **1989**, *28*, 272.
44. Tsukuda, T.; Suzuki, T.; Kaizaki, S. *Dalton Trans.* **2002**, 1721.
45. Sutter, J. P.; Kahn, M. L.; Golhen, S.; Ouahab, L.; Kahn, O. *Chem.-Eur. J.* **1998**, *4*, 571.
46. Xu, J. X.; Ma, Y.; Liao, D. Z.; Xu, G. F.; Tang, J. K.; Wang, C.; Zhou, N.; Yan, S. P.; Cheng, P.; Li, L. C. *Inorg. Chem.* **2009**, *48*, 8890.
47. Caneschi, A.; Dei, A.; Gatteschi, D.; Sorace, L.; Vostrikova, K. *Angew. Chem.-Int. Edit.* **2000**, *39*, 246.

TOC Figure

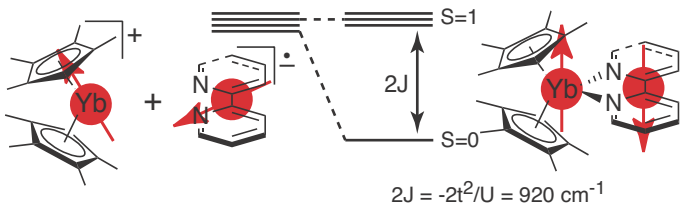

Exchange coupling has been quantified in lanthanide complexes including lanthanide single molecule magnets and $Cp^*_2Yb(bipy)$ and modeled using a Hubbard molecule model.

DISCLAIMER

DE-AC02-05CH11231